Optimization of treating phenol from wastewater through the TiO₂-catalyzed advanced oxidation process and response surface methodology

**Camila Oliveira Guimarães · Alexandre Boscaro França ·
Gisella Rossana Lamas Samanamud · Eduardo Prado Baston ·
Renata Carolina Zanetti Lofrano · Carla Cristina Almeida Loures ·
Luzia Lima Rezende Naves · Fabiano Luiz Naves**

Abstract The use of dispersed catalysts in aqueous medium inside reactors in advanced oxidative processes is common among researchers. However, due to the difficult separation of these species after treatment, in many cases, the treatment process is unfeasible. In this context, the main target of the work was the evaluation of degradation of the phenolic solution by ozonation titanium dioxide (TiO₂/P25), supported on zeolite spheres. The process was investigated through the response surface methodology (RSM) and optimized by the generalized reduced gradient (GRG) algorithm. The effects of various operating parameters including pH, power ozone (O₃) generation, flow rate, and treatment time were investigated, using as a response to removal of chemical oxygen demand (COD). It was made in optimum conditions the ratio of biochemical oxygen demand (BOD)/chemical oxygen demand to check the increasing biodegradability, aiming ozonation as preliminary treatment, with the possibility of subsequent biological treatments. There was an increase in this ratio from 0.17 to 0.50 in 48 min, which would facilitate the use of the subsequent biological process. The proposed model showed good fit to the experimental data with R^2 and R^2_{adj} correlation coefficients of 0.9964 and 0.9932, respectively.

Keywords Ozonation · Phenol · AOP · Optimization

C. Oliveira Guimarães · A. Boscaro França ·
E. Prado Baston · R. C. Zanetti Lofrano · F. L. Naves (✉)
Chemical Engineering Department, Federal University of São
João Del Rei, São João Del Rei, MG, Brazil
e-mail: fabianonavesengenheiro@ufsj.edu.br

G. R. Lamas Samanamud
Department of Civil and Environmental Engineering, University
of Texas, UTSA, San Antonio, TX 78249, USA

C. C. Almeida Loures
Department of Mechanical Engineering (DEPMC), Federal Center
for Technological Education, Angra dos Reis, RJ, Brazil

L. L. Rezende Naves
University Center of Lavras, UNILAVRAS, Lavras, MG, Brazil

Introduction

High phenol concentrations are commonly found in wastewater of petrochemical refinery processes and cooking plant, from 200 to 1500 mg L^{-1} (El-Ashtoukhy et al. 2013; Lin et al. 2011). The high toxicity of this compound may cause irreversible damages to human beings as muscle weakness, convulsions, and loss of coordination (Parish 2013). Furthermore, an acute exposition may result in blood changes, kidneys, and liver failure and even death (Parish 2013). Due to it, the Environmental Protection Agency (EPA) subject this compound to specific discharge regulations. In mineral and potable water, the concentration of phenol must be lower than 0.5 ppb and regarding wastewater fulfill its content has a limit of 0.5 ppm for surface waters and 1 ppm for the sewerage system (El-Ashtoukhy et al. 2013). Phenolic compounds have several applications

and are extensively used in industries of plastic, synthetic resins, pharmaceutical, and others (He et al. 2008).

The feature of recalcitrant phenol regardless of their concentration in an aqueous environment conducts the treatment forms that differ from the conventional. Therefore, the advanced oxidation processes (AOPs) are a possible pathway for the degradation of phenolic compounds, looking for a potential mineralization (Moussavi et al. 2009). This process is based on the oxidation of compounds by hydroxyl radicals, which are generated from common oxidants such as O_3 (Moussavi and Mahmoudi 2009). The study of ozonation and multi-phase catalytic ozonation has been exhaustively reported in the literature, through research developed (Gonçalves et al. 2013; Hanela et al. 2015; Hassani et al. 2017; Khuntia et al. 2016; Kumar et al. 2013; Oyama et al. 2014; Poblete et al. 2017; Polat et al. 2015; Quan et al. 2017; Wang et al. 2016; Zhou et al. 2017) in addition to two-phase systems with only O_3 (Lee et al. 2014; Sánchez-Polo et al. 2002; Suzuki et al. 2015).

The major benefit of using O_3 in the AOP's systems is no dependence of additional subsequent unit operations for separating the reagent from the solution after the reaction. For example, in Fenton or photo-Fenton processes, which are effective in the treatment of certain classes of wastes, the present iron ions must be separated depending on its concentration before disposal in receptor bodies. Therefore, many researchers have experimented using biphasic reactions with O_3 or in the presence of solid catalysts (Lin et al. 1998; Poggi-Varaldo et al. 2012).

The O_3 oxidation processes have been continuously used in the treatment of phenol solutions (Qiu et al. 2014), where it is observed an increase in the diffusion of this gas when using supported catalysts. The oxidation mechanism of organic compounds through the O_3 can occur by two pathways, mainly governed by the variation of pH. The direct oxidation is assigned directly from the molecular ozone present in the solution and indirect oxidation that occurs by the formation of hydroxyl radicals (Goi et al. 2004). In reactions that take place in the presence of supported catalysts, a higher diffusion of O_3 in solution and, consequently, an increase in the gas residence time in the reaction are common (He et al. 2008). Recently, titanium dioxide (TiO_2) has been used in catalytic ozonation processes of various

types of contaminants with different structures such as dye (Koutahzadeh et al. 2016), drugs (Oyama et al. 2014), chlorinated compounds (Vahid et al. 2015), and phenol solutions (Suzuki et al. 2015).

The difficulty of treating wastewater containing phenol as the main component makes it a standard compound widely studied by researchers (Bevilaqua et al. 2002; Muhammad et al. 2008), implementing methods and models addressing the final disposition within the control parameters monitored by environmental agencies (Fernando and Zapata 2012). Typically, many factors may affect directly or indirectly in the treatment of solutions containing phenol.

In this context, statistical practices for the development and optimization of models, such as response surface methodology (Ahmadzadeh and Dolatabadi 2018a, b), have been widely used in order to select levels and factors which are able of enhancing the degradation of this compound (Arslan-Alaton et al. 2009; de Sales et al. 2013; Khayet et al. 2011), such as pH, O_3 flow, time, and power of O_3 generation, as well as the interactions. This is because response surface methodology (RSM) has the construction capability models that can then be optimized from the estimated coefficients of this model. Furthermore, the bend model check, which indicates the choice of the levels, has been satisfactory for experimentation (Naves et al. 2017). In this study, the response surface methodology was used to construct the chemical oxygen demand (COD) removal model referenced to the factors already mentioned as well as algorithm (GRG) to maximize the removal of COD was used.

Materials and methods

Materials

Titanium dioxide P25 (supplied by Evonik) with specific surface area of 50 m^2 g^{-1} and composition of 70% anatase and 30% rutile (active allotropic form). Porous zeolite spheres were purchased from Sera with 5 mm average diameter. Phenol stock solution of 1.0 g L^{-1} and the total volume of 10 L were prepared using distilled water and phenol crystals (99% ACS, Vetec). The stock solution (0.1 mol L^{-1}), of H_2SO_4 and NaOH, were used to control the pH of the solution during the treatment process.

Experimental procedure

Experimental reactor

Some research has used tubular reactors where the chemical reaction can occur in a controlled manner (Hassan et al. 2016; Koutahzadeh et al. 2016). In this research, acrylic cylindrical bath reactor was based on the fixed bed theory using porous zeolite spheres (5 mm average diameter), impregnated with TiO_2 catalyst (Fig. 1). The O_3 generator equipment consists in an adjustable electric discharge of 8 kV that corresponds to 220 W of power with an outlet of O_3 linked to a flow meter with a maximum capacity of 15.0 L min^{-1}. The inlet gas is carried out in the bottom of the reactor cylinder through one spherical dispersing bubble under 14 psi of pressure.

Catalyst preparation

A suspension mixture of acetone, acrylic resin (PMMA), and TiO_2/P25 (Evonik) was prepared with a ratio of 200 mL:10.0 g:5.0 g, respectively, in which the zeolite spheres were immersed under stirring for 20 min at 50 rpm and 40 °C (Falk 2013). The spheres were removed from the suspension and dried at 130 ± 10 °C for 2 h. Finally, the spheres were washed with deionized water and dried at 120 °C during 10 h.

Catalyst characterization

The catalyst was characterized by a qualitative analysis using X-ray diffractometer (Rigaku Multiflex Diffractometer equipment) operating with $CuK\alpha$ (l = 1.5406 Å) radiation.

Experimental design and analysis procedure

The degradation effect of phenol was measured by the analysis of organic load that remained at the end of the treatment using COD, in triplicates, using the closed reflux method inferred by Standard Methods (Standard Methods for the Examination of Water and Wastewater 2012). The analyzed factors used were pH, O_3 concentration, O_3 flow rate, and time. A 1.0 g L^{-1} of phenol solution was prepared. The removal efficiency was determined based on Eq. (1).

$$COD_{\text{removal}} = \frac{COD_0 - COD_t}{COD_0} \times 100 \qquad (1)$$

where COD_0 represents the initial organic load measured without treatment and COD_t represents the organic load at time t. To analyze and validate the treatment process, the following statistical tools were used: RSM, analysis of variance (ANOVA), and hypothesis test. The response surface can be modeled through a second-order polynomial (Li et al. 2015)

$$y(x) = \beta_0 + \sum_{i=1}^{k} \beta_i x_i + \sum_{i=1}^{k} \beta_{ii} x_i^2 \qquad (2)$$
$$+ \sum_{i<j} \sum \beta_{ij} x_i x_j + \varepsilon$$

where $y(x)$ is the response, x_i is the coded values of independent variables, β_i is the regression coefficients (estimated by RSM), k is the number of independent variables, and ε is the random error. The actual values of process variables and their variation limits with its respective coding are shown in Table 1.

The ozone concentration was determined by the power of the equipment emanated from a transformer with a capacity of 220 W, as in Fig. 2.

Results and discussion

X-ray diffraction

Figure 3 shows two X-ray diffraction patterns of the zeolite spheres, with and without impregnation of TiO_2/P25. TiO_2-supported catalyst displayed well-resolved diffraction peaks (between 10 and 40 ° (2)). The existence of the peaks at 25.0°, 35.5°, 36.6°, and 37.5° (2) represents the presence of TiO_2 anatase phase type matching with JCPDS no. 21-1272. The peak at 27.8° (2) indicates the presence to the rutile phase. Moreover, the diffractograms of the support do not show any peak related to crystalline zeolite phase, which indicates that it is constituted by small crystallites (< 4 nm).

Evaluation process reduction of COD

To improve the efficiency of ozone decomposition into the AOP, high specific surface area, stability, and lower loss heterogeneous catalysts play a major role. It is
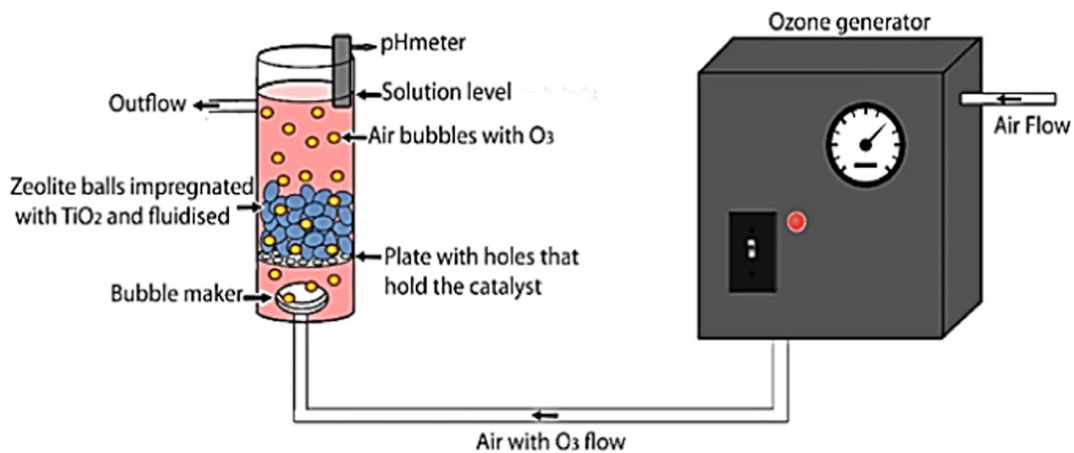
Fig. 1 Schematic design of the fluidized bed reactor with linked ozonator

important to mention that the efficiency of ozonation process using catalysts depends on, mainly, the catalyst type and its surface properties as well as the pH of the solution.

According to Ernst et al. (2004), the degradation process occurs first by the adsorption of dissolved ozone on the catalyst surface and then decomposes (rapidly) due to the presence of surface hydroxyl groups. This characteristic shows between the catalysts' promoted ozonation reaction and non-catalytic one. Applying TiO_2/zeolite catalyst, an improvement in the phenol degradation is observed.

The formation of darker color by-products, such as quinones and hydroquinones throughout the process, indicate the degradation of the phenol solution (Fig. 4).

The appearance of compounds of the quinone and hydroquinone class was determined from strong evidence of the mechanism of reduction of the organic load during the reaction, one of the first compounds to be formed over the cycle (Kondrakov et al. 2014). The

experimental results that represent the organic load reduction can be observed at RSM matrix in Table 2.

The use of the reaction time as an independent factor might be of keen interest regarding the analyses of the final costs especially concerning to O_3 use once it is only generated at high voltages.

According to Table 2, it is possible to observe some low COD reductions that are associated with minor reaction times. The phenol degradation using the ozonation process can be even less efficient when catalysts are not used. The phenol degradation process efficiency using ozonation mechanism achieved results close to 10% of the reduction in 1 h (Suzuki et al. 2015). However, when UV radiation was used with O_3, the authors could observe an increase of approximately 70% in the degradation of the phenol solution, measured by COD analyses (Suzuki et al. 2015). Therefore, there is a power consumption using UV lamp with ozone increasing the cost of the treatment process, which directs the new studies for the use of catalysts.
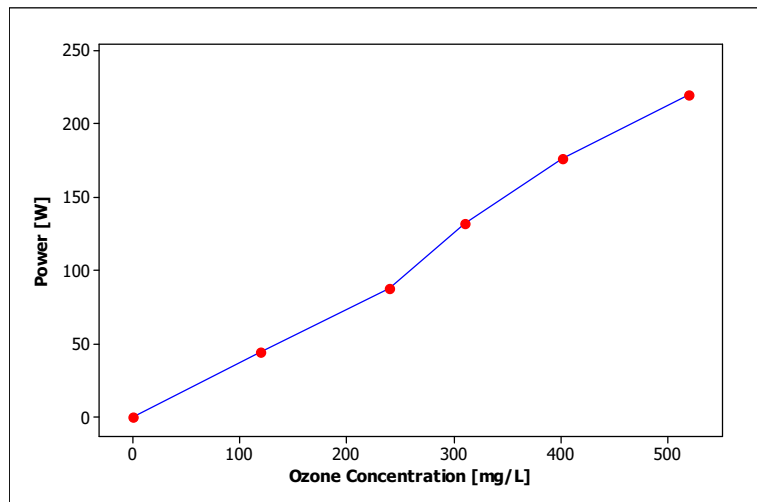
Aiming an increase in the degradation of phenol present in solution but abstaining the use of UV radiation, in this work, a model was built from the coefficients determined by the RSM regression analysis with a score R_{adj} of 0.9932 in a level of significance of 95%. Thus, through the model optimization, it was possible to find the highest phenol reduction value stipulated by the optimum factor levels. The model coefficients as its individual standard error and the p value are presented in Table 3.

Hence, a quadratic model could be described using the coefficients of Table 3 for further optimization, and it is given by Eq. (3).

Table 1 Experimental factors and level of CCD design

Factors	Range and levels (coded)				
	− 2	− 1	0	1	2
pH	3	5	7	9	11
Ozonator power [W]	77	110	143	176	209
O_3 flow rate [L min^{-1}]	1	2	3	4	5
Time [min]	15	30	45	60	75

Fig. 2 The curve of power of an ozone concentration

$$\%COD_{red} = 9.314 + 1.697*A + 6.726*B \qquad (3)$$
$$-0.506*C + 3.912*D - 0.637*A^2 + 1.343*B^2$$
$$+0.427*C^2 + 1.044*D^2 + 1.873*A*B - 0.206*A*C$$
$$-0.057*A*D - 0.590*B*C$$
$$+2.366*B*D + 1.231*C*D$$

where A, B, C, and D are the independent factors pH, ozonator power, O_3 flow rate, and reaction time, respectively, and (% COD_{red}) the percentage of organic load degradation removed of the solution. Along with the analysis of variance, it is possible to verify which factors were significant in the phenol degradation process and the quality of the final model fit, which can be made according to Table 4.

Removing from the complete model the interactions that presented a lack of significance since its p values at Table 4 exceeded the significance level of 0.05, the score R_{adj} increased to 0.933 showing an improvement in fit quality. Accordingly, the model that is going to be used in the optimization process can be redefined as Eq. (4).
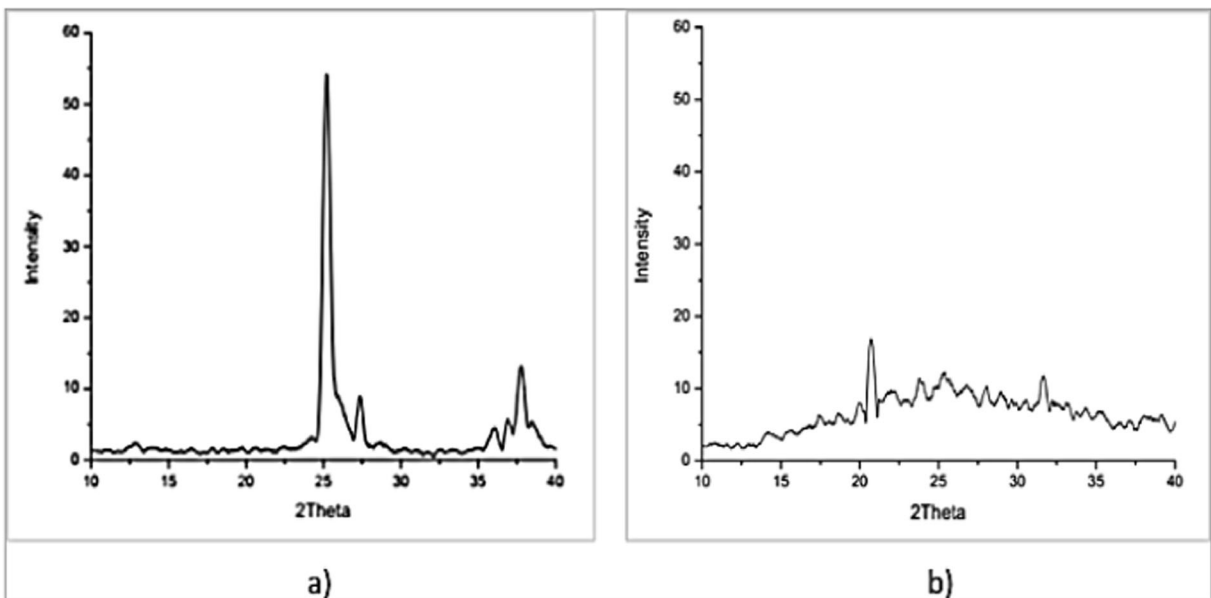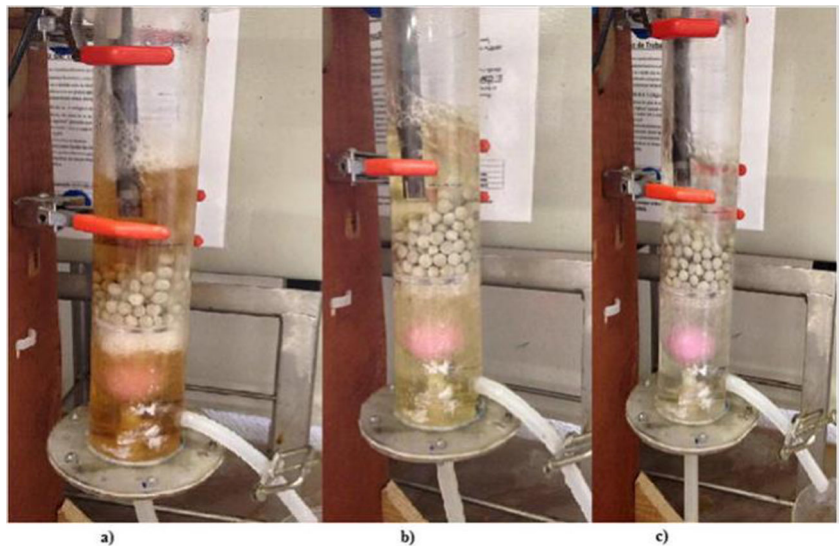

Fig. 3 X-ray diffraction. **a** TiO$_2$ impregnated over zeolite support. **b** Zeolite support

Fig. 4 Treatment of phenol solution **a** after 1 h, **b** after 2 h, **c** and after 3 h
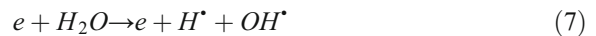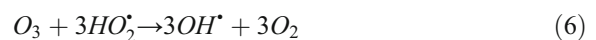

$$\%COD_{red} = 9.314 + 1.697*A$$
$$+ 6.726*B - 0.506*C$$
$$+ 3.912*D - 0.637*A^2 + 1.343*B^2$$
$$+ 0.427*C^2 + 1.044*D^2$$
$$+ 1.873*A*B - 0.590*B*C$$
$$+ 2.366*B*D + 1.231*C*D \qquad (4)$$

Another main feature in building models using experimental data is the uniformity of the residuals along the Gauss normal distribution. Using the Anderson-Darling test for residual normality, it resulted in a normal distribution from the p value metric and its value was upper the significant level of 0.05, as shown in Fig. 5.

From Eq. (4), a surface plot was built associated with a contour plot for pH × power factors that interact with each other according to Table 4. These plots can be observed in Figs. 6 and 7.

Analyzing Figs. 6 and 7, it shows that a higher organic load reduction is observed in regions of high pH and ozonator power values. According to Tang et al. (2009), a raise in the ozonator power increases the hydroxyl radical production indirectly because of the higher production of O_3 as shown in Eqs. (5–6). Besides that, when the power is increased, the electrons gain more energy in the electric field raising the ionization of water and oxygen molecules by collision inside the DBD reactor according to Eqs. (7–8) (Tang et al.

2009). The gas source used in this experiment has a relative humidity of 54%.

$$OH^- + O_3 \rightarrow {}^{\bullet}O_2^- + HO_2^{\bullet} \qquad (5)$$

$$O_3 + 3HO_2^{\bullet} \rightarrow 3OH^{\bullet} + 3O_2 \qquad (6)$$

$$e + H_2O \rightarrow e + H^{\bullet} + OH^{\bullet} \qquad (7)$$

$$O\left({}^1D\right) + H_2O \rightarrow 2OH^{\bullet} \qquad (8)$$

Meantime, an enhancement of the power from 60 to 127 W might lead to a considerable reduction of these radicals because when this input power is increased to a certain level, it might occur formation of UV radiation and NO_x production (Tang et al. 2009). According to Kogelschatz (2003), the UV radiation influences the number of micro-discharges per unit of electrode area and cycle. Therefore, the change in the operating parameter (power) affects the discharge mode once the nature of the micro-discharge changes due to UV formation (Kogelschatz 2003). After that, the micro-discharge frequency also changes because for a given configuration and fixed peak voltage, the power is directly proportional to the frequency (Kogelschatz 2003; Tang et al. 2009). An excessive power increases the concentration level of NO/NO_2 which enhances the NO_x reactions that consume oxygen atoms at a faster rate than the ozone

Table 2 CCD matrix with its levels and COD removal response

	pH	Power [W]	Flow rate [L min^{-1}]	Time [min]	COD reduction [%]
1	5	110	2	30	4.474
2	9	110	2	30	4.008
3	5	176	2	30	10.595
4	9	176	2	30	17.305
5	5	110	4	30	1.811
6	9	110	4	30	1.737
7	5	176	4	30	5.696
8	9	176	4	30	12.819
9	5	110	2	60	4.877
10	9	110	2	60	4.923
11	5	176	2	60	20.110
12	9	176	2	60	28.305
13	5	110	4	60	8.317
14	9	110	4	60	6.670
15	5	176	4	60	21.409
16	9	176	4	60	27.200
17	3	143	3	45	3.452
18	11	143	3	45	10.980
19	7	77	3	45	1.433
20	7	209	3	45	28.837
21	7	143	1	45	12.273
22	7	143	5	45	10.670
23	7	143	3	15	6.306
24	7	143	3	75	21.570
25	7	143	3	45	9.574
26	7	143	3	45	9.638
27	7	143	3	45	9.335
28	7	143	3	45	8.239
29	7	143	3	45	9.200
30	7	143	3	45	9.853
31	7	143	3	45	9.358

formation reaction in Eqs. (9–11) that may cause the reduction of (HO$^{\bullet}$) radical formation rate.

$$N^{\bullet} + O_3 \rightarrow NO + O_2 \tag{9}$$

$$NO + O_3 \rightarrow NO_2 + O_2 \tag{10}$$

$$N_2\left(A^3\textstyle\sum\right) + H_2O \rightarrow N_2 + OH^{\bullet} + H^{\bullet} \tag{11}$$

According to Li et al. (2015), the hydroxyl radical formation during the degradation process of phenol solution is potentiated at basic pH, more precisely upper to 9. The O$_3$ production rate (mg s^{-1}) can be calculated using Eq. (12), which is closely linked to the cost of energy (J) demanded by the equipment according to Eq. (13) (Tichonovas et al. 2013).

$$A = \frac{C_{\text{ozone}} \times Q_{\text{gás}}}{60} \tag{12}$$

$$E = \frac{P \times 48000}{A \times 6.022 \times 10^{23}} \tag{13}$$

where P is the reactor discharge power (W).

Table 3 Coefficients, individual standard error, and p value

Factors	Coefficients	SE coefficients	p value
Constant	9.314	0.2422	0.000
pH	1.697*	0.1308	0.000
Power	6.726*	0.1308	0.000
Flow rate	− 0.506*	0.1308	0.001
Time	3.912*	0.1308	0.000
pH × pH	− 0.637*	0.1198	0.000
Power × power	1.343*	0.1198	0.000
Flow rate × flow rate	0.427*	0.1198	0.003
Time × time	1.044*	0.1198	0.000
pH × power	1.873*	0.1602	0.000
pH × flow rate	− 0.206	0.1602	0.218
pH × time	− 0.057	0.1602	0.728
Power × flow rate	− 0.590*	0.1602	0.002
Power × time	2.366*	0.1602	0.000
Flow rate × time	1.231*	0.1602	0.000

*Significant coefficients to model (p value < 0.05)

The interaction also significant of flow rate × power of ozonator is directly related to the O_3 mass transfer inside the reactor. High flow rates of gas lead to a reduction in the mass transfer due to the lower residence time feature by the formation of larger bubbles. Thus, if the power is raised, it favors the direct oxidation mechanism that is made by O_3 directly. In Figs. 8 and 9, it is possible to observe this interaction.

In Figs. 8 and 9, it can be noted that an extensive range of flow rate, 1.0 to 5.0 L min^{-1}, favors the phenol degradation together with the power factor. A gradual increase in the removal of COD from 5% to more than 25% shows the major influence of the ozonator power. It is important to note that when the power is kept constant, an enhancement in the flow rate decreases the degradation percentage of phenol in a solution that is justified by the lower in the mass transfer of the gas inside the reactor.

Biodegradability relationship

Considering the application of the ozonation process as a pre-treatment of a high degree of recalcitrance waste,

Table 4 Variance analyses (ANOVA)

Source	DF	Seq SS	Adj SS	Adj MS	F	p
Regression	14	1803.75	1803.75	128.84	313.69	0.000
Linear	4	1528.40	1528.40	382.10	930.31	0.000
pH	1	69.13	69.13	69.13	168.32	0.000
Power	1	1085.80	1085.80	1085.80	2643.65	0.000
Flow rate	1	6.14	6.14	6.14	14.96	0.001
Time	1	367.31	367.31	367.31	894.31	0.000
Square	4	99.15	99.15	24.79	60.35	0.000
pH × pH	1	22.97	11.60	11.60	28.23	0.000
Power × power	1	42.15	51.57	51.57	125.57	0.000
Flow rate × flow rate	1	2.89	5.21	5.21	12.69	0.003
Time × time	1	31.15	31.15	31.15	75.83	0.000
Interaction	6	176.20	176.20	29.37	71.50	0.000
pH × power	1	56.10	56.10	56.10	136.59	0.000
pH × flow rate	1	0.68	0.68	0.68	1.65	0.218
pH × time	1	0.05	0.05	0.05	0.13	0.728
Power × flow rate	1	5.57	5.57	5.57	13.57	0.002
Power × time	1	89.55	89.55	89.55	218.03	0.000
Flow rate × time	1	24.25	24.25	24.25	59.04	0.000
Residual error	16	6.57	6.57	0.41		
Lack-of-fit	10	4.94	4.94	0.49	1.81	0.241
Pure error	6	1.63	1.63	0.27		
Total	30	1810.32				

Fig. 5 The Anderson-Darling test for residual distribution
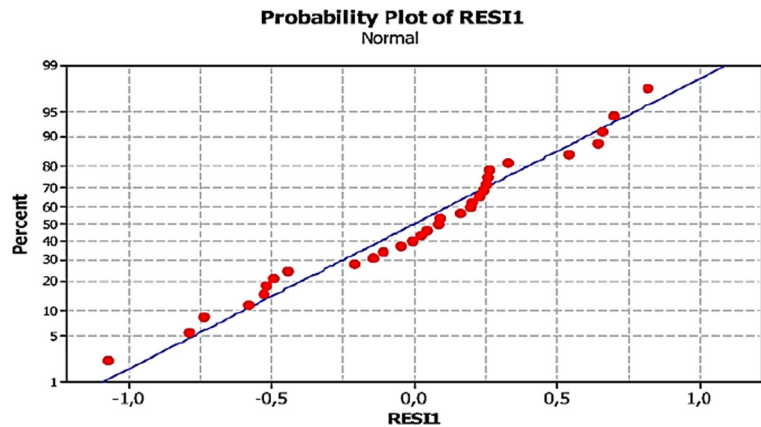
reducing this property can further facilitate the use of biological treatment procedures, which are conventional and easy to handle. However, the basic restriction on the utilization of this type of treatment is the sensitivity of the bacteria and protozoa to this organic compounds, which can be measured by two metrics: chemical oxygen demand and biological oxygen demand, the reason these quantities indicate the operating capacity of a biological station. According to Tina (2015)), the bio-degradability of waste may be measured by this relationship, the contextualization of the use or non-biological processes according to Table 5.

Although COD removal was achieved in the optimized conditions of 36%, BOD/COD ratio before and after treatment experienced an increase from 0.17 to 0.40, showing that after treatment time, phenol solution could be transferred to biological treatment (Table 6).

Model optimization and validation

The model was optimized by the algorithm generalized reduced gradient (GRG), and it was validated using the statistical test 1-sample-*t* which comprises in a mean comparison test of COD removal percentage between

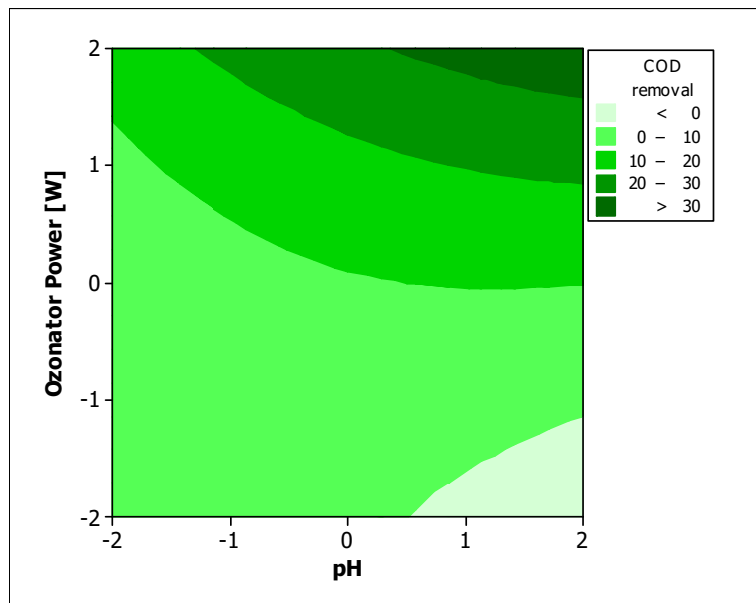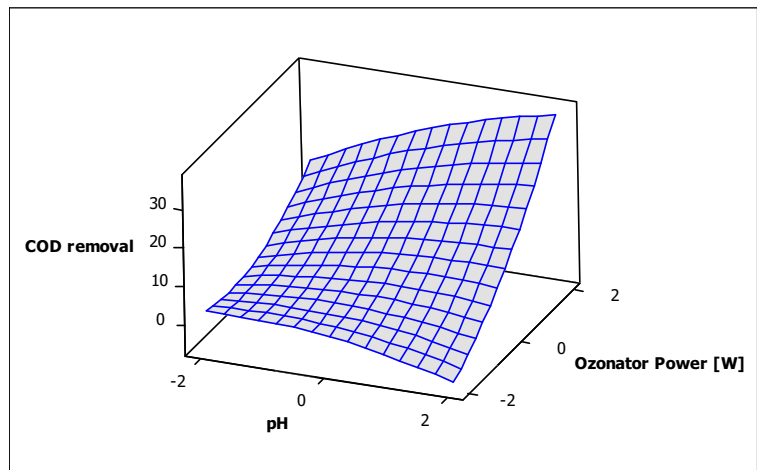**Fig. 6** Contour plot of %COD removal vs. pH; power

Fig. 7 Surface plot of %COD removal vs. pH; power of ozonator

the values predicted by the model and the experimental ones. The optimization based on lab scale might support the implementation for industrial output. Hence, it is crucial to creating and validate models that represent and that minimize the instability of real processes in a reliable way.

In this context, using the coefficients obtained from the response surface methodology (model) on the GRG algorithm of Excel software, the optimum coded levels of each experimental factor were determined. From the linear relation between coded and uncoded values as exposed in Eq. (4), the uncoded values could be determined based on the already known relation between those values previously presented in Table 7.
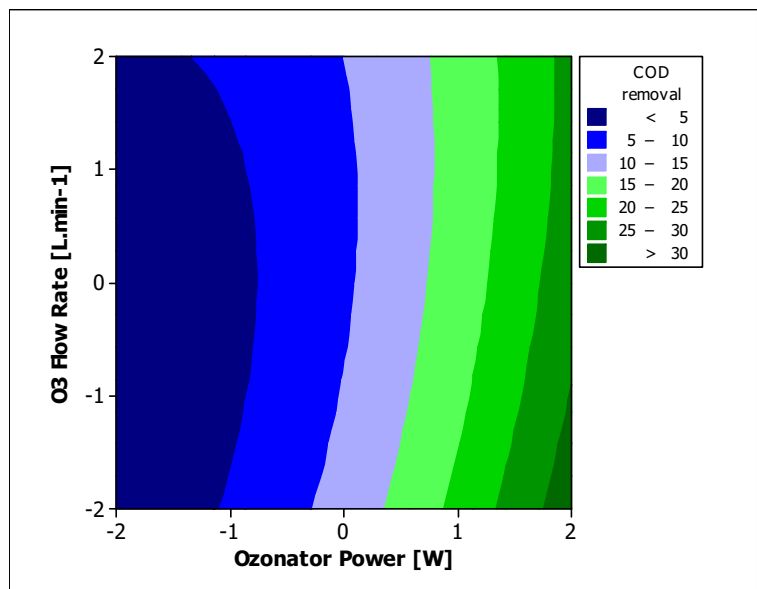
Higher pH values expedite the phenol degradation through the catalytic ozonation once it leads to more dissociated fractions which are more prone to be oxidized by O_3 (Marotta et al. 2012). In this way, pH 7.5 was determined from the optimized conditions. Marota et al. used the ozonation process in phenol solution treatment and taking a range of pH between 1.9 and 10.1 found pH 7 as the optimum value during the reactions. According to the previous Eqs. (5–6), the O_3 decomposition to form $HO^{\bullet}$ just occurs at high pH values. However, the optimum pH value determined is a neutral-basic pH. The presence of water on the gas source makes possible the occurrence of Eqs. (3–4), also showed previously. Therefore, it is important to notice that the optimum point calls

Fig. 8 Contour plot of %COD removal vs. flow; power

Fig. 9 Surface plot of %COD removal vs. flow; power
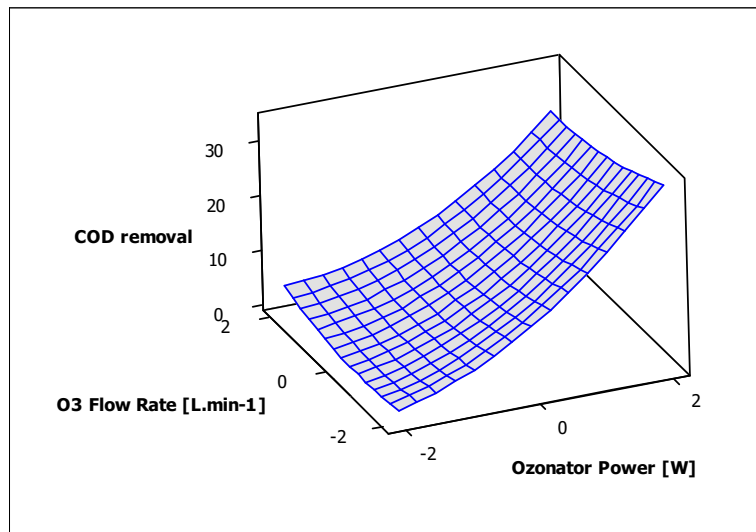
for an equilibrium between variables. Hence, there is no need to control the system at high pH levels which would lead to spend in more chemicals, if there is maintenance of reasonable power values permitting the formation of HO$^{\bullet}$ from other sources.

The polynomial built from the response surface plus the optimum levels already discussed resulted in a COD reduction value of 25.62%. Regarding the 1-sample-t test, it was determined the adequate amount of experiments linked to the reproducibility and repeatability. For this purpose, the power and sample size test was used through the software Minitab returning some three replicates to validate the model, as can be seen in Fig. 10.

The three experimental replicates were done at the optimized level conditions as Table 5 and the COD values were determined for each of the replicates, as presented in Table 8.

The experimental COD reduction values were then compared to the predicted value obtained from the model. Therefore, using a hypothesis test according to Eqs. (6–7), a p value of 0.89 was obtained that is a higher value than the level of significance 0.05. This result

leads to the acceptance of null hypothesis that comprises in the equality of the average COD reductions: experimental and predicted by the model.

$$H_0 : \mu_{predita} = \mu_{experimental}$$

$$H_1 : \mu_{predita} \neq \mu_{experimental}$$

where $\mu_{predita}$ and $\mu_{experimental}$ are, respectively, the average COD reductions predicted and experimental.

It was also carried out a verification test on catalyst efficiency ozonation process. The COD removal in optimal conditions without the catalyst was around 23%. In contrast in the presence of the catalyst, there was a substantial increase of 13%, from about 36% removal.

According to the discussed above, due to the high density of hydroxyl groups on the TiO$_2$/zeolite catalyst, active atomic oxygen is produced and reacted with zeolite hydroxyl surface groups to form O$_2$H$^-$ anions which subsequently can react very fast with another O$_3$ to form O$_2$H$^{\bullet}$ radicals or the O$_2$H$^-$ radicals can be produced directly. This radical reacts subsequently with

Table 5 Biodegradability and BOD/COD ratio (Tina 2015)

BOD/COD	Biodegradability of the substance
Values higher than 0.6	Totally biodegradable
Values between 0.41 and 0.59	Partially biodegradable
Values less than 0.4	Not biodegradable

Table 6 Biodegradability and BOD/COD ratio

Response	Beginning	After 48 min of treatments
DBO [mgO$_2$ L^{-1}]	201	385
DQO [mgO$_2$ L^{-1}]	1134	771
DBO/DQO	0.17	0.50

Table 7 The coded and uncoded optimum conditions

Factors	pH	Power (W)	Flow rate (L min^{-1})	Time (min)
Optimum coded values	0.317	1.143	0	0.768
Optimum uncoded values	7.5	178	3	58

Table 8 COD experimental reduction

COD reduction %	26.784	29.341	30.108
Experimental mean		28.744 ± 1.740	

another ozone molecule to generate an O_3^- radical. The O_3^- radical decomposes into oxygen and a free $HO^{\bullet}$ radical which can oxidize organic compounds either in solution or on the surface or in a thin film layer on the surface of the catalyst.

The amount of adsorption was also studied, i.e., an experiment was conducted only with the phenol solution and the catalyst, without the presence of ozone to the environment. In this context, there was a small change in the COD removal of only 2.2%, which sets a COD removing percentage with the catalyst from Eq. (14).

$$D(\%) = R_{cc} - R_{sc} - R_{ads}$$
$$D(\%) = 36 - 23 - 2.2 \qquad (14)$$
$$D(\%) = 10.8\%$$

At where:

D (%)	total difference with and without use of catalyst use
R_{cc}	removal with catalyst
R_{wc}	COD removal without catalyst
R_{ads}	COD removal by adsorption of phenol solution the zeolite beads

Another aspect that explains the participation of catalyst in the decomposition reaction of the organic matter from the phenol in solution indicates that for zeolites having a density of large pores, conditioning in pores with smaller diameters, usually fisiosorção phenomenon is low, indicating that diffusion in the pores to be limiting process step (Levenspiel 1999). Another fact that illustrates the presence of chemisorption along the reaction is that the change in the molar flow of ozone within the reactor alters the degradation of phenol in the solution, which indicates the presence of chemisorption (Levenspiel 1999).

Conclusions

The use of ozone in the treatment of phenol solution may be a large step, especially since pre-treatment. Therefore, the efficiency can be increased gradually with the use of catalysts as herein the impregnated titanium dioxide based on the zeolite. The removal of COD in the optimized conditions was only 36% in 48 min sufficient for removing this increased biodegradability of the phenol solution. The use of the catalyst conditioned a difference in reduction in COD of 13%, and contextualization using trailers catalysts the use of ozone in advanced oxidation processes, a promising

Fig. 10 Test power and sample size

source of partial decontamination or complete on directly to the treatment time, and can, therefore, be tested on larger scales aiming industrial use. The factors pH, ozonator power, O_3 flow rate, and reaction time proved to be significant in the phenol solution degradation that could be referenced and proven according to the literature, as well as the interactions.

References

Ahmadzadeh, S., & Dolatabadi, M. (2018a). In situ generation of hydroxyl radical for efficient degradation of 2,4-dichlorophenol from aqueous solutions. *Environmental Monitoring and Assessment, 190*(6). https://doi.org/10.1007/s10661-018-6697-0.

Ahmadzadeh, S., & Dolatabadi, M. (2018b). Modeling and kinetics study of electrochemical peroxidation process for mineralization of bisphenol A; a new paradigm for groundwater treatment. *Journal of Molecular Liquids, 254*, 76–82. https://doi.org/10.1016/j.molliq.2018.01.080.

Arslan-Alaton, I., Tureli, G., & Olmez-Hanci, T. (2009). Treatment of azo dye production wastewaters using photo-Fenton-like advanced oxidation processes: optimization by response surface methodology. *Journal of Photochemistry and Photobiology A: Chemistry, 202*(2–3), 142–153. https://doi.org/10.1016/j.jphotochem.2008.11.019.

Bevilaqua, J. V., Cammarota, M. C., Freire, D. M. G., & Sant'Anna, G. L. (2002). Phenol removal through combined biological and enzymatic treatments. *Brazilian Journal of Chemical Engineering, 19*(2), 151–158. https://doi.org/10.1590/S0104-66322002000200010.

de Sales, P. F., Magriotis, Z. M., Rossi, M. a. L. S., Resende, R. F., & Nunes, C. a. (2013). Optimization by response surface methodology of the adsorption of Coomassie Blue dye on natural and acid-treated clays. *Journal of Environmental Management, 130*, 417–428. https://doi.org/10.1016/j.jenvman.2013.08.067.

El-Ashtoukhy, E. S. Z., El-Taweel, Y. A., Abdelwahab, O., & Nassef, E. M. (2013). Treatment of petrochemical wastewater containing phenolic compounds by electrocoagulation using a fixed bed electrochemical reactor. *International Journal of Electrochemical Science, 8*(1), 1534–1550.

Ernst, M., Lurot, F., & Schrotter, J. C. (2004). Catalytic ozonation of refractory organic model compounds in aqueous solution by aluminum oxide. *Applied Catalysis B: Environmental, 47*(1), 15–25. https://doi.org/10.1016/S0926-3373(03)00290-X.

Falk, G. da S. (2013). *Impregnação de Tio2 Em Esponja Cerâmica Para Aplicações Fotocatalíticas* (pp. 1–66).

Fernando, C., & Zapata, V. (2012). *Modelo Simplificado Para a Transferência De Massa No Processo De Ozonização Em Uma Coluna De Borbulhamento*. Campinas: Unicamp.

Goi, A., Trapido, M., & Tuhkanen, T. (2004). A study of toxicity, biodegradability, and some by-products of ozonised nitrophenols. *Advances in Environmental Research, 8*(3–4), 303–311. https://doi.org/10.1016/S1093-0191(02)00102-8.

Gonçalves, A. G., Órfão, J. J. M., & Pereira, M. F. R. (2013). Ceria dispersed on carbon materials for the catalytic ozonation of

sulfamethoxazole. *Journal of Environmental Chemical Engineering, 1*(3), 260–269. https://doi.org/10.1016/j.jece.2013.05.009.

Hanela, S., Durán, J., & Jacobo, S. (2015). Removal of iron–cyanide complexes from wastewaters by combined UV–ozone and modified zeolite treatment. *Journal of Environmental Chemical Engineering, 3*(3), 1794–1801. https://doi.org/10.1016/j.jece.2015.06.023.

Hassan, M., Zhao, Y., & Xie, B. (2016). Employing TiO2 photocatalysis to deal with landfill leachate: current status and development. *Chemical Engineering Journal, 285*, 264–275. https://doi.org/10.1016/j.cej.2015.09.093.

Hassani, A., Khataee, A., Karaca, S., & Fathinia, M. (2017). Degradation of mixture of three pharmaceuticals by photocatalytic ozonation in the presence of TiO2/montmorillonite nanocomposite: simultaneous determination and intermediates identification. *Journal of Environmental Chemical Engineering, 5*(2), 1964–1976. https://doi.org/10.1016/j.jece.2017.03.032.

He, K., Dong, Y. M., Li, Z., Yin, L., Zhang, A. M., & Zheng, Y. C. (2008). Catalytic ozonation of phenol in water with natural brucite and magnesia. *Journal of Hazardous Materials, 159*(2–3), 587–592. https://doi.org/10.1016/j.jhazmat.2008.02.061.

Khayet, M., Zahrim, A. Y., & Hilal, N. (2011). Modelling and optimization of coagulation of highly concentrated industrial grade leather dye by response surface methodology. *Chemical Engineering Journal, 167*(1), 77–83. https://doi.org/10.1016/j.cej.2010.11.108.

Khuntia, S., Majumder, S. K., & Ghosh, P. (2016). Catalytic ozonation of dye in a microbubble system: hydroxyl radical contribution and effect of salt. *Journal of Environmental Chemical Engineering, 4*(2), 2250–2258. https://doi.org/10.1016/j.jece.2016.04.005.

Kogelschatz, U. (2003). Dielectric-barrier discharges: their history, discharge physics, and industrial applications. *Plasma Chemistry and Plasma Processing, 23*(1), 1–46. https://doi.org/10.1023/A:1022470901385.

Kondrakov, A. O., Ignatev, A. N., Frimmel, F. H., Bräse, S., Horn, H., & Revelsky, A. I. (2014). Formation of genotoxic quinones during bisphenol A degradation by TiO2 photocatalysis and UV photolysis: a comparative study. *Applied Catalysis B: Environmental, 160–161*(1), 106–114. https://doi.org/10.1016/j.apcatb.2014.05.007.

Koutahzadeh, N., Esfahani, M. R., & Arce, P. E. (2016). Removal of acid black 1 from water by the pulsed corona discharge advanced oxidation method. *Journal of Water Process Engineering, 10*, 1–8. https://doi.org/10.1016/j.jwpe.2016.01.010.

Kumar, P., Agnihotri, R., & Mondal, M. K. (2013). Catalytic treatment of synthetic dye wastewater: COD and color reduction. *Journal of Environmental Chemical Engineering, 1*(3), 440–447. https://doi.org/10.1016/j.jece.2013.06.008.

Lee, Y., Kovalova, L., McArdell, C. S., & von Gunten, U. (2014). Prediction of micropollutant elimination during ozonation of a hospital wastewater effluent. *Water Research, 64*, 134–148. https://doi.org/10.1016/j.watres.2014.06.027.

Levenspiel, O. (1999). Chemical Reaction Engineering, Industrial & Engineering Chemistry Research. https://doi.org/10.1021/ie990488g.

Li, G., Lu, Y. T., Lu, C., Zhu, M. S., Zhai, C. Y., Du, Y. K., & Yang, P. (2015). Efficient catalytic ozonation of bisphenol-A

over reduced graphene oxide modified sea urchin-like alpha-MnO2 architectures. *Journal of Hazardous Materials, 294*, 201–208. https://doi.org/10.1016/j.jhazmat.2015.03.045.

Lin, S. H., Shyu, C. T., & Sun, M. C. (1998). Saline wastewater treatment by electrochemical method. *Water Research, 32*(4), 1059–1066. https://doi.org/10.1016/S0043-1354(97)00327-8.

Lin, S.-H., Chiou, C.-H., Chang, C.-K., & Juang, R.-S. (2011). Photocatalytic degradation of phenol on different phases of TiO2 particles in aqueous suspensions under UV irradiation. *Journal of Environmental Management, 92*(12), 3098–3104. https://doi.org/10.1016/j.jenvman.2011.07.024.

Marotta, E., Ceriani, E., Schiorlin, M., Ceretta, C., & Paradisi, C. (2012). Comparison of the rates of phenol advanced oxidation in deionized and tap water within a dielectric barrier discharge reactor. *Water Research, 46*(19), 6239–6246. https://doi.org/10.1016/j.watres.2012.08.022.

Moussavi, G., & Mahmoudi, M. (2009). Degradation and biodegradability improvement of the reactive red 198 azo dye using catalytic ozonation with MgO nanocrystals. *Chemical Engineering Journal, 152*(1), 1–7. https://doi.org/10.1016/j.cej.2009.03.014.

Moussavi, G., Khavanin, A., & Alizadeh, R. (2009). The investigation of catalytic ozonation and integrated catalytic ozonation/biological processes for the removal of phenol from saline wastewaters. *Journal of Hazardous Materials, 171*(1–3), 175–181. https://doi.org/10.1016/j.jhazmat.2009.05.113.

Muhammad, A., Shafeeq, A., Butt, M. A., Rizvi, Z. H., Chughtai, M. A., & Rehman, S. (2008). Decolorization and removal of COD and BOD from raw and biotreated textile dye bath effluent through advanced oxidation processes (AOPS). *Brazilian Journal of Chemical Engineering, 25*(3), 453–459. https://doi.org/10.1590/S0104-66322008000300003.

Naves, F. L., de Paula, T. I., Balestrassi, P. P., Moreira Braga, W. L., Sawhney, R. S., & de Paiva, A. P. (2017). Multivariate normal boundary intersection based on rotated factor scores: a multiobjective optimization method for methyl orange treatment. *Journal of Cleaner Production, 143*, 413–439. https://doi.org/10.1016/j.jclepro.2016.12.092.

Oyama, T., Otsu, T., Hidano, Y., Tsukamoto, T., Serpone, N., & Hidaka, H. (2014). Remediation of aquatic environments contaminated with hydrophilic and lipophilic pharmaceuticals by TiO2-photoassisted ozonation. *Journal of Environmental Chemical Engineering, 2*(1), 84–89. https://doi.org/10.1016/j.jece.2013.11.008.

Parish, C. (2013). *Agency for toxic substances and disease registry.* https://www.atsdr.cdc.gov/index.html. Accessed 24 Sept 2016.

Poblete, R., Oller, I., Maldonado, M. I., Luna, Y., & Cortes, E. (2017). Cost estimation of COD and color removal from landfill leachate using combined coffee-waste based activated carbon with advanced oxidation processes. *Journal of Environmental Chemical Engineering, 5*(1), 114–121. https://doi.org/10.1016/j.jece.2016.11.023.

Poggi-Varaldo, H. M., Bárcenas-Torres, J. D., Moreno-Medina, C. U., García-Mena, J., Garibay-Orijel, C., Ríos-Leal, E., & Rinderknecht-Seijas, N. (2012). Influence of discontinuing feeding degradable cosubstrate on the performance of a fluidized bed bioreactor treating a mixture of trichlorophenol and phenol. *Journal of Environmental Management, 113*, 527–537. https://doi.org/10.1016/j.jenvman.2012.03.015.

Polat, D., Balcı, İ., & Özbelge, T. A. (2015). Catalytic ozonation of an industrial textile wastewater in a heterogeneous continuous reactor. *Journal of Environmental Chemical Engineering, 3*(3), 1860–1871. https://doi.org/10.1016/j.jece.2015.04.020.

Qiu, C., Yuan, S., Li, X., Wang, H., Bakheet, B., Komarneni, S., & Wang, Y. (2014). Investigation of the synergistic effects for p-nitrophenol mineralization by a combined process of ozonation and electrolysis using a boron-doped diamond anode. *Journal of Hazardous Materials, 280*, 644–653. https://doi.org/10.1016/j.jhazmat.2014.09.001.

Quan, X., Luo, D., Wu, J., Li, R., Cheng, W., & Ge, s. (2017). Ozonation of acid red 18 wastewater using O3/Ca(OH)2 system in a micro bubble gas-liquid reactor. *Journal of Environmental Chemical Engineering, 5*(1), 283–291. https://doi.org/10.1016/j.jece.2016.12.007.

Sánchez-Polo, M., Rivera-Utrilla, J., & Zaror, C. a. (2002). Advanced oxidation with ozone of 1,3,6-naphthalenetrisulfonic acid in aqueous solution. *Journal of Chemical Technology and Biotechnology, 77*(2), 148–154. https://doi.org/10.1002/jctb.539.

Standard Methods for the Examination of Water and Wastewater. (2012). *Standard Methods.* 20th edition. https://doi.org/10.2105/AJPH.51.6.940-a.

Suzuki, H., Araki, S., & Yamamoto, H. (2015). Evaluation of advanced oxidation processes (AOP) using O3, UV, and TiO2 for the degradation of phenol in water. *Journal of Water Process Engineering, 7*, 54–60. https://doi.org/10.1016/j.jwpe.2015.04.011.

Tang, Q., Jiang, W., Zhang, Y., Wei, W., & Lim, T. M. (2009). Degradation of azo dye acid red 88 by gas phase dielectric barrier discharges. *Plasma Chemistry and Plasma Processing, 29*(4), 291–305. https://doi.org/10.1007/s11090-009-9181-3.

Tichonovas, M., Krugly, E., Racys, V., Hippler, R., Kauneliene, V., Stasiulaitiene, I., & Martuzevicius, D. (2013). Degradation of various textile dyes as wastewater pollutants under dielectric barrier discharge plasma treatment. *Chemical Engineering Journal, 229*, 9–19. https://doi.org/10.1016/j.cej.2013.05.095.

Tina, K. (2015). *BPA performance (TOC, BOD and toxicity) during photo-Fenton reaction.* Lahti: Lahti University of Applied Sciences.

Vahid, B., Mousanejad, T., & Khataee, A. (2015). Sonocatalytic ozonation, with nano-TiO2 as catalyst, for degradation of 4-chloronitrobenzene in aqueous solution. *Research on Chemical Intermediates, 41*(10), 7029–7042. https://doi.org/10.1007/s11164-014-1796-1.

Wang, Y., Yang, W., Yin, X., & Liu, Y. (2016). The role of Mn-doping for catalytic ozonation of phenol using Mn/γ-Al2O3 nanocatalyst: performance and mechanism. *Journal of Environmental Chemical Engineering, 4*(3), 3415–3425. https://doi.org/10.1016/j.jece.2016.07.016.

Zhou, Q., Wang, Q., & Tong, S. (2017). Mn2+/H2O2/O3, a high efficient advanced oxidation process in acidic solution. *Journal of Environmental Chemical Engineering, 5*(1), 924–930. https://doi.org/10.1016/j.jece.2017.01.002.